Electron-excited $4d \rightarrow 4f$ Ba resonances in $YBa_2Cu_3O_{7-\delta}$: Selection rules at intermediate electron energy

C. W. Clark
Radiation Physics Division, National Institute of Standards and Technology, Gaithersburg, Maryland 20899

J. A. D. Matthew
Department of Physics, University of York, Heslington, York Y01 5DD, England

M. G. Ramsey and F. P. Netzer
Institut für Physikalische Chemie, Universität Innsbruck, A-6020 Innsbruck, Austria

(Received 13 July 1989)

Observations of electron-excited $4d^{10}4f^0 \rightarrow 4d^9 4f^1$ giant resonances of Ba in the high-T_c superconductor $YBa_2Cu_3O_{7-\delta}$ are compared with previous work on the corresponding La transition in various environments. Breakdown of dipole selection rules is observed even at electron primary energies of a few keV, but for low-angle scattering it is possible to rationalize the results in terms of symmetry-related selection and intensity rules appropriate to intermediate coupling. This interpretation is supported by atomic Hartree-Fock calculations of the final-state multiplets.

It has long been known that electron excitation of atoms and quasiatomic systems does not follow the strict dipole selection rule of photon excitation, and giant resonances[1] involving $4d \rightarrow 4f$ excitations in the elemental range Ba–Yb provide a particularly interesting test of the applicability of generalized selection rules. Netzer, Strasser, and Matthew[2] used electron-energy-loss spectroscopy (EELS) to show that $4d^{10}4f^0 \rightarrow 4d^9(4f^1, ef^1)$ transitions in La were quasiatomic in character and insensitive to environment. The number of multiplets excited below the main $^1P^\circ$ dipole resonance steadily increased as the primary energy decreased from 2 keV, at which only a few optically forbidden transitions are observed, to 300 eV, at which a large number of $4d^9 4f^1$ states appear. These observations were confirmed by Moser *et al.*[3] and Onsgaard, Jansson, and Andersen,[4] while Strasser *et al.*[5] followed the effect through the rare-earth series. Electron excitation of the similar giant resonance transition in Ba has received little attention, but is of interest due to the fact that the giant resonance phenomenon in Ba is known to be highly sensitive to the ionic state. Although extensive photoabsorption studies of Ba have resulted in a fairly complete description of $4d^9 nf^1$ states with $J = 1$, odd parity,[6] there have been no resolved observations of states of different symmetry in these configurations. A comprehensive account of the $4d^9 4f^1$ configuration would be of particular interest, since theoretical investigations of neighboring Cs have shown the presence of radical orbital term dependence.[7]

The present study of the giant resonances in EELS of Ba in the high-T_c superconducting system $YBa_2Cu_3O_{7-\delta}$ is intended primarily to address the above issues. Since we focus on a localized phenomenon dominated by the core hole potential at the Ba site, we do not expect to uncover any information directly relevant to the mechanism of high-temperature superconductivity. Our analysis does, however, provide some insight into the valency of Ba in this compound (it is close to +2), which may be relevant to speculations regarding the effect of the Ba ionic polarizability upon the superconducting transition temperature.[8]

The experimental setup has been described in a previous EELS study of the lower-energy excitations ($E < 50$ eV) of high-T_c superconductors.[9] The $YBa_2Cu_3O_{7-\delta}$ sample had a transition temperature onset at 90 K and transition width of a few degrees, though these properties were not crucial to the study presented here. EELS spectra were recorded on a VG ADES 400 electron spectrometer with hemispherical analyzer (resolution 0.3–0.4 eV), and the samples were cleaned by scraping in UHV with a corundum file.

Figure 1 shows the EELS spectrum of Ba in $YBa_2Cu_3O_{7-\delta}$ for a wide range of primary energies. At low primary energies a cluster of relatively sharp peaks in the loss spectrum is observed between 90 and 100 eV; as the primary energy increases, the excitation strength in this region of energy loss becomes concentrated in two features, at ~95 and 98 eV. As we show below, the sharp peaks can be attributed to states of the $4d^9 4f^1$ configuration (closed subshells not indicated), all of which—with the notable exception of $^1P_1^\circ$—are highly localized states whose characteristics are insensitive to the chemical environment of the Ba atom. The $4d^9 4f^1\,{}^1P_1^\circ$ state, on the other hand, is a Rydberg state in the free Ba atom, due to the strong repulsive dipole exchange potential in the $4d^9 \epsilon f^1\,{}^1P_1^\circ$ channel. The repulsive potential gives rise to a continuum-shape resonance, in which most of the dipole oscillator strength is concentrated. This "giant" resonance corresponds to the broad peak at 105-eV loss energy. The giant resonance has a highly localized component, similar to the $4d^9 4f^1$ non-$^1P_1^\circ$ states, which is not sensitive to the Ba environment.

Thus the energy of the resonance is approximately the same in the free Ba atom and ions, Ba metal, and the various molecular compounds that have been studied. However, its mode of decay can be quite dependent upon its surroundings; for example; in going from Ba to Ba^{2+} in the gas phase, the $4d$ ionization limit is raised above the resonance energy, so that the resonance is actually distributed throughout a discrete Rydberg portion of the $4d$ excitation spectrum.[10,11] In the nominal "Ba^{2+}" associated with the halides BaX_2, this resonance appears notably sharper than in the atom or the metal, and exhibits excitonic structure which corresponds to the strong $4f^9nf$ lines observed in gas-phase Ba^{2+}. The second broad peak at ~120-eV loss energy is also observed in photoabsorption by Ba in various environments. Its energy does not depend strongly upon Ba valency, so it must be associated with a localized, atomiclike final state. We attribute this peak to $4d^{10}5p^6 \rightarrow 4d^9 5p^5 5d^2$ excitation. Our calculations place several states of the excited configuration in the correct energy range, and indicate that they can acquire significant oscillator strength from interaction with the $4d^9 5p^6 \epsilon f$ channel. The strength in photoabsorption of this feature relative to that of the 105-eV giant resonance depends strongly on the valence of Ba. In atomic Ba the giant resonance is clearly dominant, but the relative strength of the second peak in the BaX_2 halides increases with the electronegativity of X, so that in BaF_2 the two features are almost twins. The relative strengths of our EELS peaks at the higher primary energies are consistent with those observed in total photoyield experiments on this compound,[12,13] which supports the argument that Ba exists in a +2 valence state similar to that of $BaBr_2$.

We now discuss the low- and high-energy-loss spectra in somewhat more detail. The inset to Fig. 1 shows a simple model for the low-energy-loss spectrum, in which the cross section for excitation of a state of the $4d^9 4f^1$ configuration is supposed to be proportional to its statistical weight. The energies of all states (except $^1P_1^\circ$) of this configuration in Ba^{2+} have been computed in the single-configuration approximation with intermediate coupling using Cowan's code,[14] and have been placed on an absolute scale by setting the computed energy of the $^3D_1^\circ$ state equal to the value of 94.55 eV determined from photoabsorption measurements on the free Ba^{2+} ion.[11] A plausible but arbitrary Gaussian width of 1 eV has been imposed on each state. Given the simplicity of the model and the relatively low resolution of the experimental spectra, we have not thought it meaningful to attempt to improve the agreement between them by adjusting the

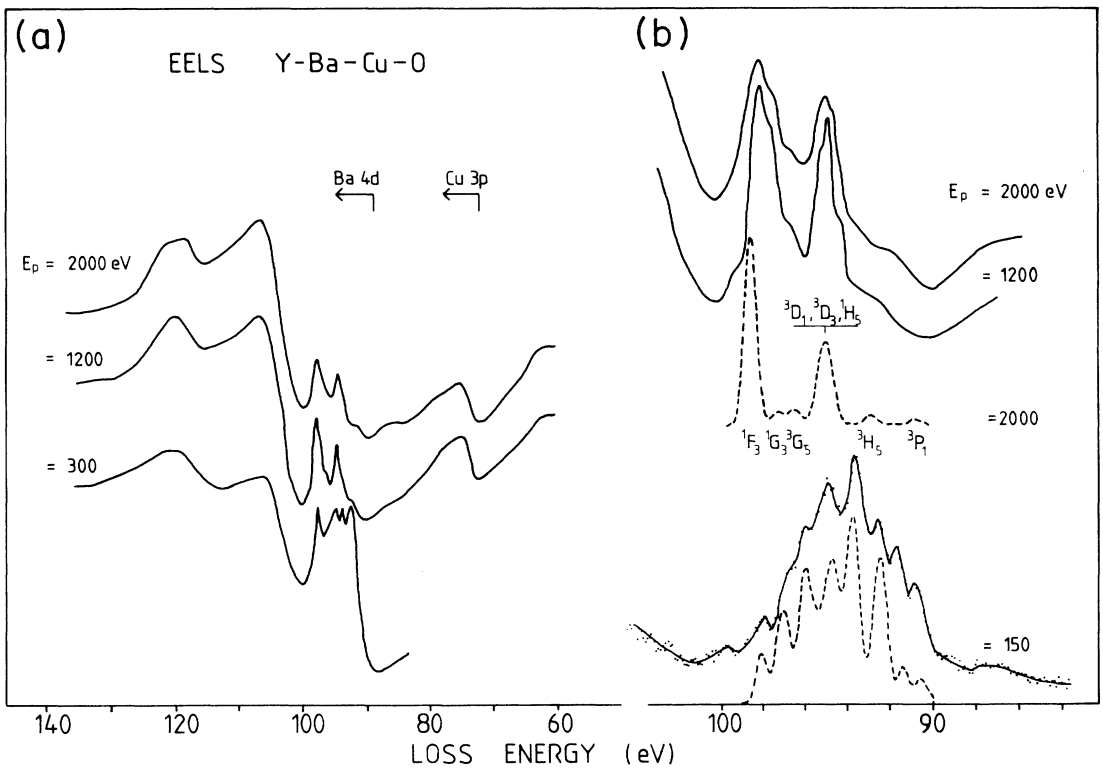

FIG. 1. (a) EELS spectra in the region of Ba $4d$ excitations as a function of the incident electron energy. (b) The region of the sharp multiplets below the $4d$ ionization limit, with an expanded energy scale. The bottom spectrum ($E_p = 150$ eV) shows both the data points and the smoothed curve to indicate the statistics. The dashed curve beneath the 150-eV spectrum shows a model low-energy-loss spectrum for $4d^{10}4f^0 \rightarrow 4d^9 4f^1$ excitation, which assumes the excitation cross section to be proportional to the statistical weight of the final state, as described in the text. The dashed curve beneath the 2-keV spectrum shows the relative integrated cross sections for these transitions as computed in the Born approximation.

parameters of the atomic Hamiltonian or the linewidths. These results certainly suggest that excitation at low primary energies is entirely nonselective, and that all $4d^9 4f^1$ states except for $^1P_1^\circ$ are present in the cluster.

As the primary energy E_p increases, the excitation strength in this region of the spectrum is dominated by two features at 95 and 98 eV. We treat these features along the lines used by Netzer, Strasser, and Matthew[2] in the analysis of EELS of La. When the primary energy E_p is more than ~ 10 times the energy loss, it is reasonable to describe the inelastic collision by the first Born approximation. We have found it useful to discuss this approximation in terms of the generalized oscillator strength, using a representation developed rather elegantly in the review by Inokuti.[15] The integrated cross section σ_n for the transition $\psi_0 \rightarrow \psi_n$ excited by an incident electron of energy E_p is (in a.u.)

$$\sigma_n = \frac{2\pi}{E_p} \int_{[\ln(K^2)]_{\min}}^{[\ln(K^2)]_{\max}} d\ln(K^2) f_n(K) \Big/ 2E_n \ , \tag{1}$$

where $\mathbf{K} = \mathbf{k}_f - \mathbf{k}_i$ is the momentum transferred to the electron in the collision, E_n is the excitation energy, and the generalized oscillator strength $f_n(K)$ is given by

$$f_n(K) = 2E_n K^{-2} \sum_{j=1}^{N} |\langle \psi_n | \exp(i\mathbf{K}\cdot\mathbf{r}_j) | \psi_0 \rangle|^2 \ , \tag{2}$$

where the sum runs over all target electrons. Equation (1) is just an integration over all scattering angles; the variable $\ln(K^2)$ is convenient for graphical purposes. We now consider the high-energy spectrum in terms of elementary properties of the generalized oscillator strength.

The generalized oscillator strength clearly vanishes for spin-changing transitions, and also for those transitions in which the angular momentum and parity of the target do not change in step. Consider the expansion

$$\exp(i\mathbf{K}\cdot\mathbf{r}_j) = \sum_{L=0}^{\infty} (2L+1) i^L j_L(Kr_j) P_L(\cos(\hat{\mathbf{K}}\cdot\hat{\mathbf{r}}_j)) \ .$$

If ψ_0 is a ^1S state, the excitation of a ^1L state is mediated by the terms proportional to $P_L(\cos(\hat{\mathbf{K}}\cdot\hat{\mathbf{r}}_j))$; these transform as $(-1)^L$ under inversion of the coordinates of the target electrons. The parity of the final state produced by this excitation must thus be $(-1)^L$ that of ψ_0. For $4d^{10}4f^0 \rightarrow 4d^9 4f^1$ transitions, the final state necessarily has odd parity, as dictated by the electronic configuration. It is therefore restricted to be of $^1P_1^\circ$, $^1F_3^\circ$, or $^1H_5^\circ$ symmetry (corresponding respectively to dipole, octupole, and, for want of a better word, 2^5-pole transitions). Goddard *et al.*[16] have shown that in the particular case of axial collisions, the same selection rule derives from basic symmetry arguments and thus does depend upon the applicability of the Born approximation. The $4d^9 4f^1$ eigenstates are not characterized by pure LS coupling, so this selection rule must be interpreted as restricting the final-state angular momentum J to be odd, with the relative intensity of the transition being proportional to the weight of the ^1J component of the eigenfunction.

We have computed the generalized oscillator strengths for multipole transitions to the localized $4d^9 4f^1$ states, using Hartree-Fock configuration average orbitals for

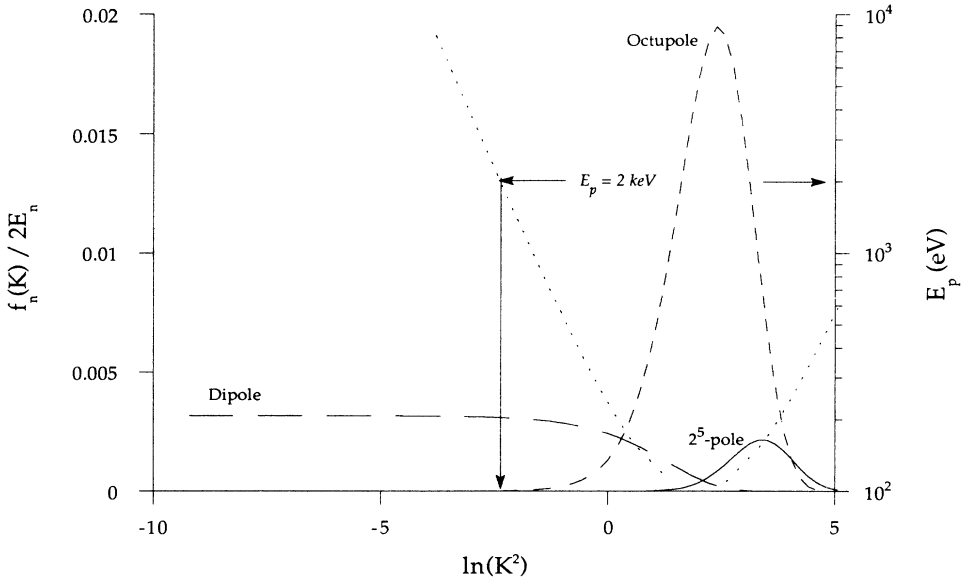

FIG. 2. Generalized oscillator strengths for transitions to the $^3D_1^\circ$ (dipole, long dash), $^1F_3^\circ$ (octupole, short dash), and $^1H_5^\circ$ (2^5-pole, solid line) states, as a function of $\ln(K^2)$, with K in atomic units. The left vertical axis gives $f_n(K)/2E_n$ [Eq. (2)] in atomic units. The relative cross sections for these transitions are proportional to the areas under their respective curves between the limits $\ln(K^2)_{\min}$ and $[\ln(K^2)]_{\max}$. These limits are represented as functions of the collision energy E_p (right vertical axis) by the dotted curves; note that the areas under the curves are effectively independent of $[\ln(K^2)]_{\max}$ for $[\ln(K^2)]_{\max} > 5$, so that the upper range of integration need not be explicitly represented. Arrows indicate the range of integration for $E_p = 2$ keV, at which the integrated $^3D_1^\circ$ cross section is $\sim \frac{1}{4}$ that of $^1F_3^\circ$.

Ba^{2+} generated by the Froese-Fischer code,[17] and intermediate-coupling coefficients from the Cowan code, as described above. Figure 2 depicts the results for the $^3D_1^\circ$, $^1F_3^\circ$, and $^1H_5^\circ$ states, which have the strongest transitions for $J=1$, 3, and 5, respectively. The generalized oscillator strengths all decrease rapidly as $\ln(K^2) \rightarrow \infty$; as $\ln(K^2) \rightarrow -\infty$, the dipole strength tends to a constant value, whereas the higher multipole strengths vanish. From Eq. (1) it is seen that the relative excitation cross section for a given transition is simply proportional to the *area* under its curve in this representation. The range of integration can be inferred from the values of $[\ln(K^2)]_{\min}$ and $[\ln(K^2)]_{\max}$ that are shown as functions of E_p.

Several straightforward observations may be made from this figure. First of all, for E_p larger than ~ 1 keV the ratio of octupole of 2^5-pole intensities is independent of E_p (since there is no further accumulation of area), and is approximately equal to 10. There is no energy at which the integrated 2^5-pole cross section exceeds that of the octupole. Secondly, the dipole strength eventually dominates the octupole with increasing E_p, since its area increases as $-[\ln(K^2)]_{\min}$. However, since $[-\ln(K^2)]_{\min} \sim \ln(2E_p) - \ln(E_n^2)$ for large E_p, this dominance occurs at very high energies: at $E_p \sim 80$ MeV, according to this calculation. At $E_p = 2$ keV the integrated octupole strength is about four times that of the dipole, as can be estimated visually from the figure. Finally, the relative intensities of dipole and octupole excitation depend critically upon intermediate coupling. The $^3D_1^\circ$ state in our approximation has only a 0.25% admixture of $^1P_1^\circ$ symmetry, and a correspondingly low dipole oscillator strength $f \sim 0.02$; if this admixture were to increase by a factor of 5, dipole excitation would always be dominant.

In EELS experiments of the type described in this paper, the detected electrons have been backscattered from the sample, and have therefore experienced at least one large-angle elastic collision in addition to the primary inelastic collision. We shall assume that this multiple scattering averages out of the effect of different angular distributions for the different multipole transitions, and therefore renders the EELS yield proportional to the integrated cross section. The inset of the 2-keV spectrum of Fig. 1(b) shows the EELS spectrum as computed from the Born approximation described above, assuming the yield to be proportional to the integrated cross section, and imposing the same 1-eV Gaussian widths upon each peak. It so happens that the $^3D_3^\circ$ state, which can be excited by an octupole transition via a small (16%) admixture of $^1F_3^\circ$, lies within 0.5 eV of the $^3D_1^\circ$ state, as does a $J=5$ state. The peak at 95 eV is thus a blend of dipole, octupole, and 2^5-pole features. The main peak at 98 eV is associated with the $^1F_3^\circ$ state. The three states with $J=5$ are better characterized by *jj* than by *LS* coupling, and the weight of the $^1H_5^\circ$ component is spread fairly evenly among them (42%, 35%, and 23%).

The $4d$ EELS spectrum of La at E_p above 1 keV exhibits its two sharp peaks similar to those observed here; the selection rules above were invoked by Netzer, Strasser, and Matthew[2] to associate the higher-energy peak with a $4d^9 4f^1\,{}^1F_3^\circ$ state, and the lower with a blend of transitions to the $^1H_5^\circ$ and $^3D_1^\circ$ states. Intermediate-coupling calculations on La (Ref. 3) reveal near degeneracy of a $J=3$ and a $J=5$ state with the $^3D_1^\circ$ state, so it is very likely that the lower peak also contains an octupole feature, as is the case in Ba. The additional small features observed by Netzer, Strasser, and Matthew[2] and by Moser *et al.*[3] are in good correspondence with the pattern presented here.

The general picture of the evolution of intensities of the $4d^{10}4f^0 \rightarrow 4d^9(4f^1, ef^1)$ transitions can be summarized as follows. For $E_p \gg E_n$ the Born approximation allows the excitation of all odd values of J. The bulk of the dipole excitation strength is concentrated in the $4d^9 ef^1$ shape resonance. In the discrete spectrum, dipole and octupole transitions are of comparable intensity up to very high energies; 2^5-pole excitation is weaker, but easily discernable. The detailed distribution of intensity is governed by intermediate coupling; as a rule, the validity of *LS* coupling decreases with increasing J, so that the multipole excitation strength gets distributed among an increasing number of states. As E_p decreases, the scattering becomes less dominated by the lowest-order Born interaction, and excitation of even values of J will become allowed. Finally, as E_p approaches threshold the Born approximation fails entirely. Transitions to all states become possible, with a pattern of relative intensity which is difficult to predict by first-principles calculations, but which follows approximately the statistical weight of the final state.

In summary we have shown that quasiatomic $4d^{10}4f^0 \rightarrow 4d^9(4f^1, ef^1)$ resonances are observed in EELS of Ba in $YBa_2Cu_3O_{7-\delta}$ with properties very similar to the corresponding transition in La metal. Remarkably we have been able to use data from a highly complex solid to help illuminate the step-by-step breakdown of selection rules for inelastic scattering of electrons by atoms. This is an unusual application of a high-T_c superconductor.

This research has been supported in part by the Fonds zur Föderung der Wissenschaftlichen Forschung of Austria, and the U.S. Air Force Office of Scientific Research. One of us (J.A.D.M.) wishes to thank the United Kingdom Science and Engineering Research Council for travel funds.

[1]See reviews of this field in *Giant Resonances in Atoms, Molecules, and Solids*, edited by J. P. Connerade, J. M. Esteva, and R. C. Karnatak (Plenum, New York, 1987).

[2]F. P. Netzer, G. Strasser, and J. A. D. Matthew, Phys. Rev. Lett. **51**, 211 (1983).

[3]H. R. Moser, B. Delley, W. D. Schneider, and Y. Baer, Phys. Rev. B **29**, 2947 (1984).

[4]J. Onsgaard, C. Jansson, and J. N. Andersen, J. Electron Spec-

trosc. Relat. Phenom. **46**, 227 (1988).
[5]G. Strasser, G. Rosina, J. A. D. Matthew, and F. P. Netzer, J. Phys. F **15**, 739 (1985).
[6]T. B. Lucatorto, T. J. McIlrath, J. Sugar, and S. M. Younger, Phys. Rev. Lett. **47**, 1124 (1984).
[7]C. W. Clark, Phys. Rev. A **35**, 4865 (1987).
[8]M. Ronay and D. M. Newns, Phys. Rev. B **39**, 819 (1989).
[9]M. G. Ramsey, F. P. Netzer, and J. A. D. Matthew, Phys. Rev. B **39**, 732 (1989).
[10]T. B. Lucatorto, T. J. McIlrath, W. T. Hill III, and C. W. Clark, in *X-Ray and Atomic Inner-Shell Physics* (University of Oregon), Proceedings of the International Conference on X-Ray and Atomic Inner-Shell Physics-1982, AIP Conference Proceedings No. 94, edited by B. Crasemann (AIP, New York, 1982), p. 584.
[11]C. W. Clark, J. Opt. Soc. Am. B **1**, 626 (1984).
[12]M. Onellion, Y. Chang, D. W. Niles, R. Joynt, G. Margarintondo, N. G. Stoffel, and J. M. Tarascon, Phys. Rev. B **36**, 819 (1987).
[13]K. L. Tsang, C. H. Zhang, T. A. Callcott, L. R. Canfield, D. L. Ederer, J. E. Blendell, C. W. Clark, N. Wassdahl, J. E. Rubensson, G. Bray, N. Mortensson, J. Nordgren, R. Nyholm, and S. Cramm, Phys. Rev. B **37**, 2293 (1988).
[14]R. Cowan, *Theory of Atomic Structure and Spectra* (University of California Press, Berkeley, 1981).
[15]M. Inokuti, Rev. Mod. Phys. **43**, 297 (1971); M. Inokuti, Y. Itikawa, and J. E. Turner, Rev. Mod. Phys. **50**, 23 (1978).
[16]W. A. Goddard III, D. L. Huestis, D. C. Cartwright, and S. Trajmar, Chem. Phys. Lett. **11**, 329 (1971).
[17]C. Froese Fischer, Comput. Phys. Commun. **14**, 145 (1978).